# FIGURES

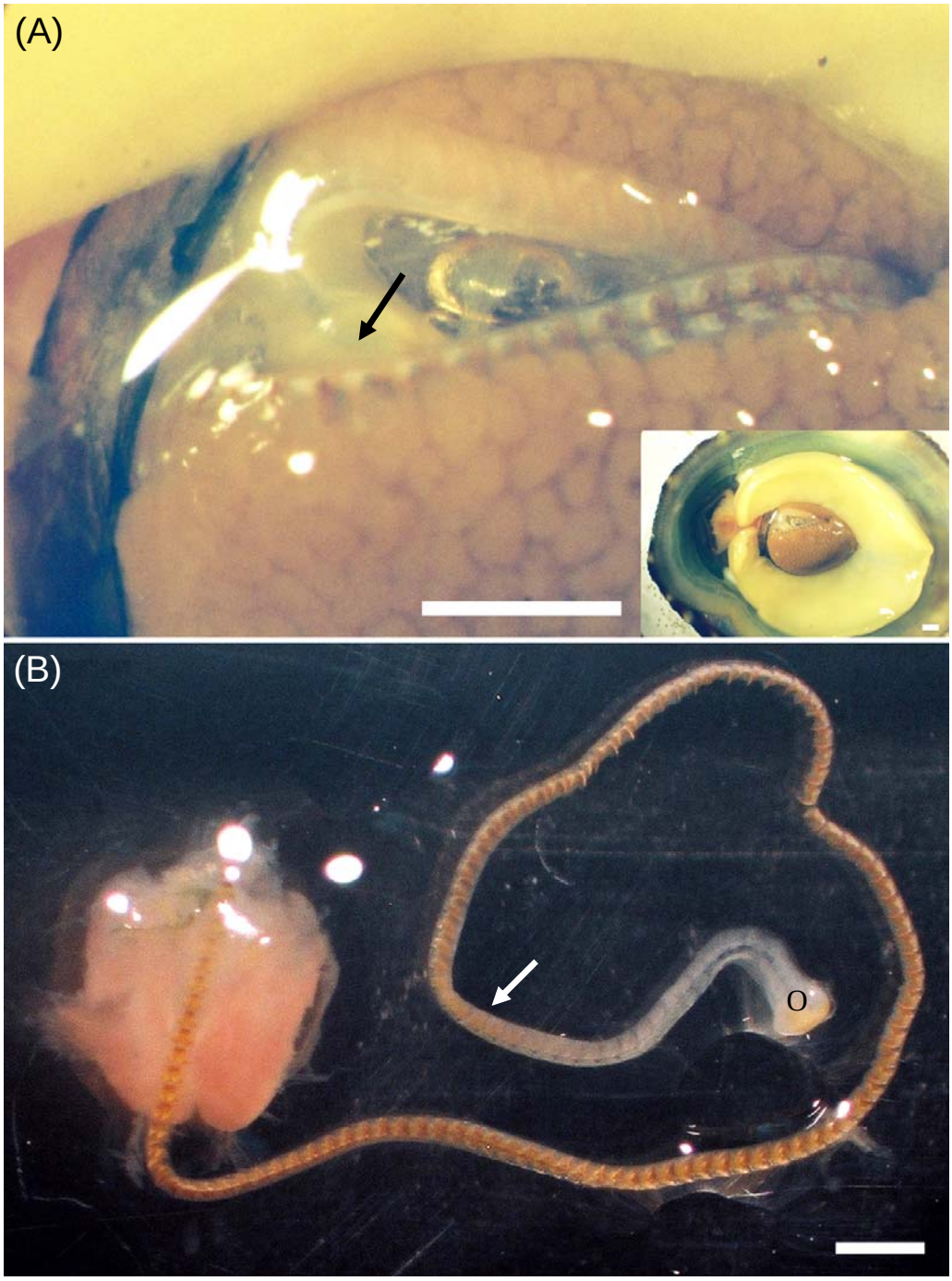


FIG. 1. The anatomy of a limpet.
(A) Removal of the abdominal foot reveals the seminal vesicle and part of the radula. Black arrow, odontoblast. (B) Complete radula removed from the limpet. Noted that stage II (white arrow) showed a redish-orange color indicating the Fe influx. O, odontoblast. Scale bar, 1 mm.

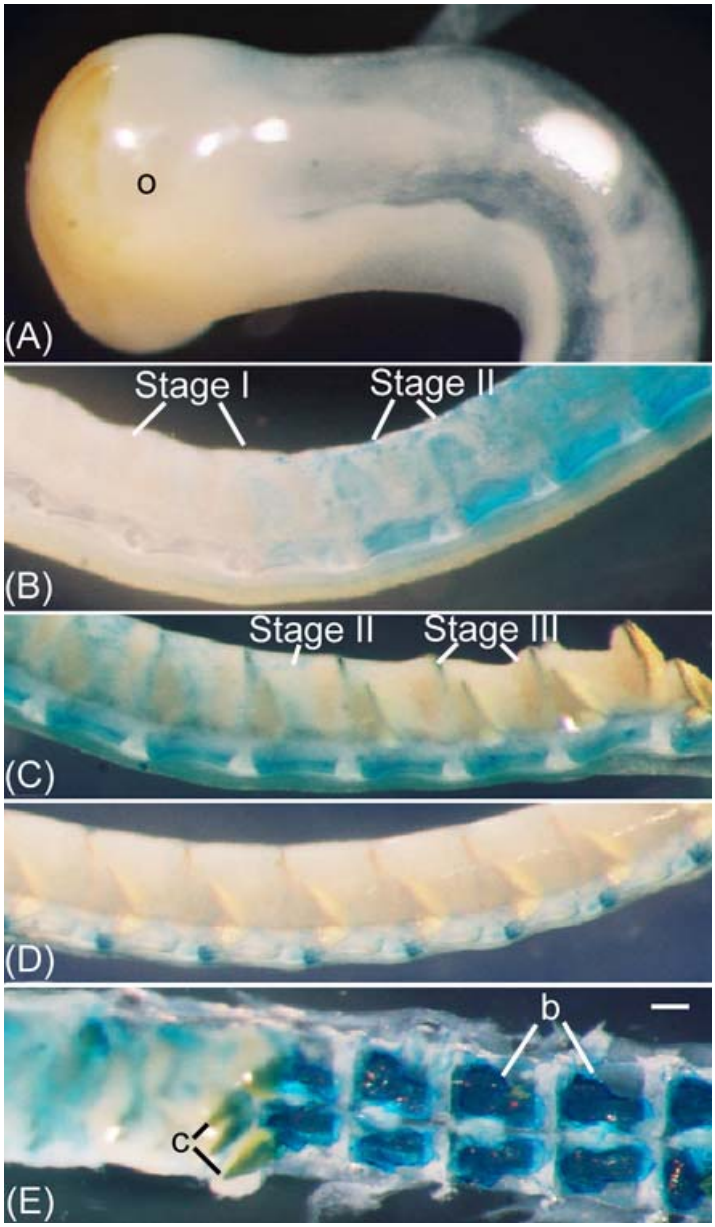


FIG. 2. Stereomicroscopic images of freshly dissected radula of *N. schrenckii* after Prussian stain.

(A) This segment contains no iron to react with the Prussian blue staining reagent, thus the color remained unaltered; O, odontoblast. (B) The boundary of stage I and stage II. Note that in stage II the epithelial cells and the tooth base stained blue in stage II. (C) Segment of late stage II and early stage III. The blue intensity of epithelial cells reduced while the color in tooth base sustained. (D) Late stage III. Only fraction of the tooth base were stained blue. The color was absent completely from the epithelial cells in this stage. (E) A fragment of stage II of which several rows of tooth cusps were peered off, revealing the heavily stained tooth base; b, base; c, cusp. Scale bar, 100 μm

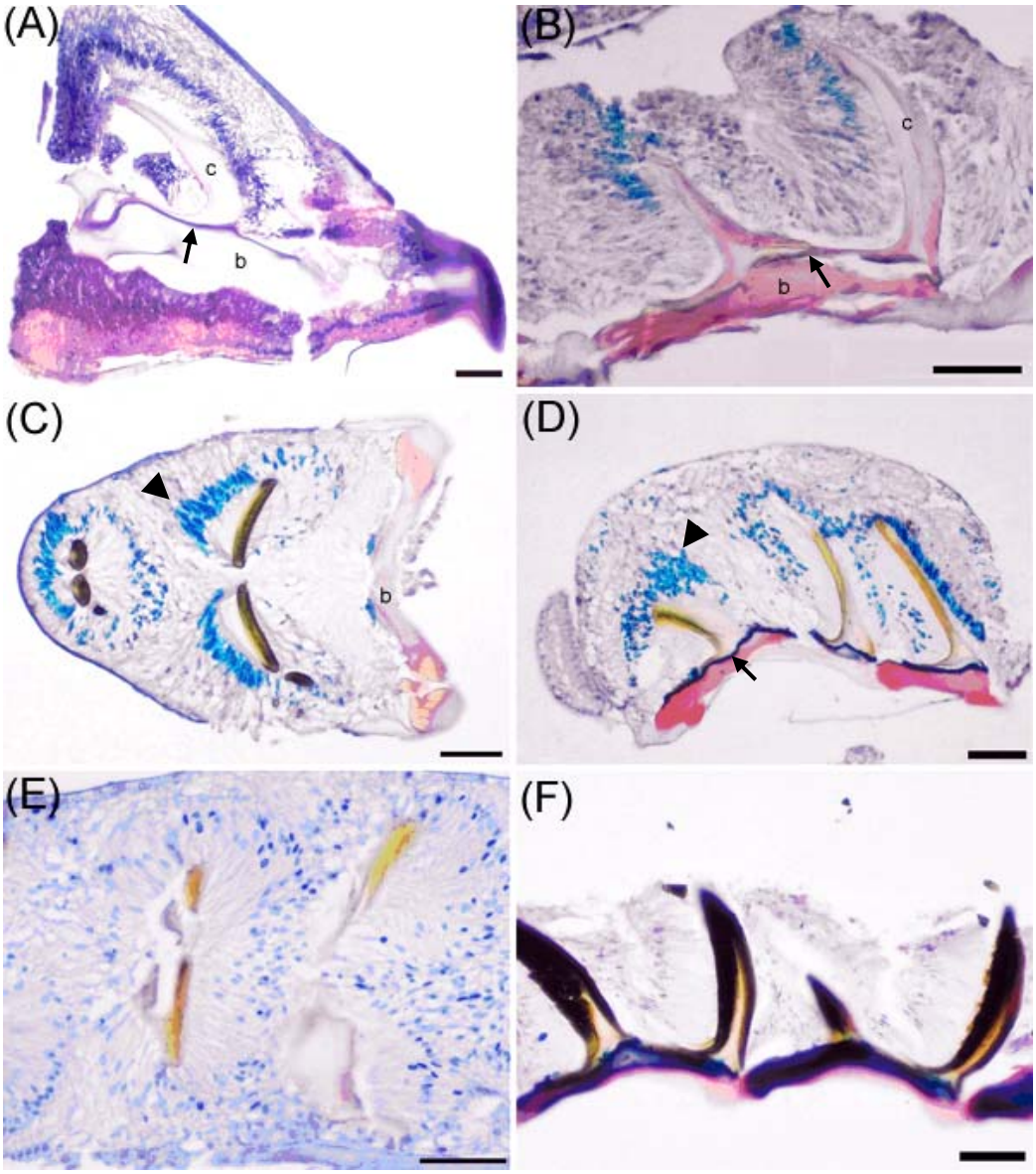


FIG. 3. Histological sections of the radula.

(A) Stage I radula along with the surrounding epithelial cells. The junction zone appears at this stage (arrow). (B) Area between late stage I and early stage II. Iron influx begins at this region. Part of the epithelial cells and the junction zone (arrow) were stained blue. (C) and (D) Cross and longitudinal sections of stage II radula. Iron was transferred to the cusp, and the mineralization began. Arrow, junction zone; arrow heads, epithelial cells involved in iron transportation. (E) Section of late stage II. Minerals deposited in the cusp can be clearly seen. The amount of iron concentration in epithelial cells begins to decline. (F) Radula with mineralization process completed. The cusp exhibited dark brown color, and almost no iron could be detected in epithelial cells. Scale bar, 100 μm.

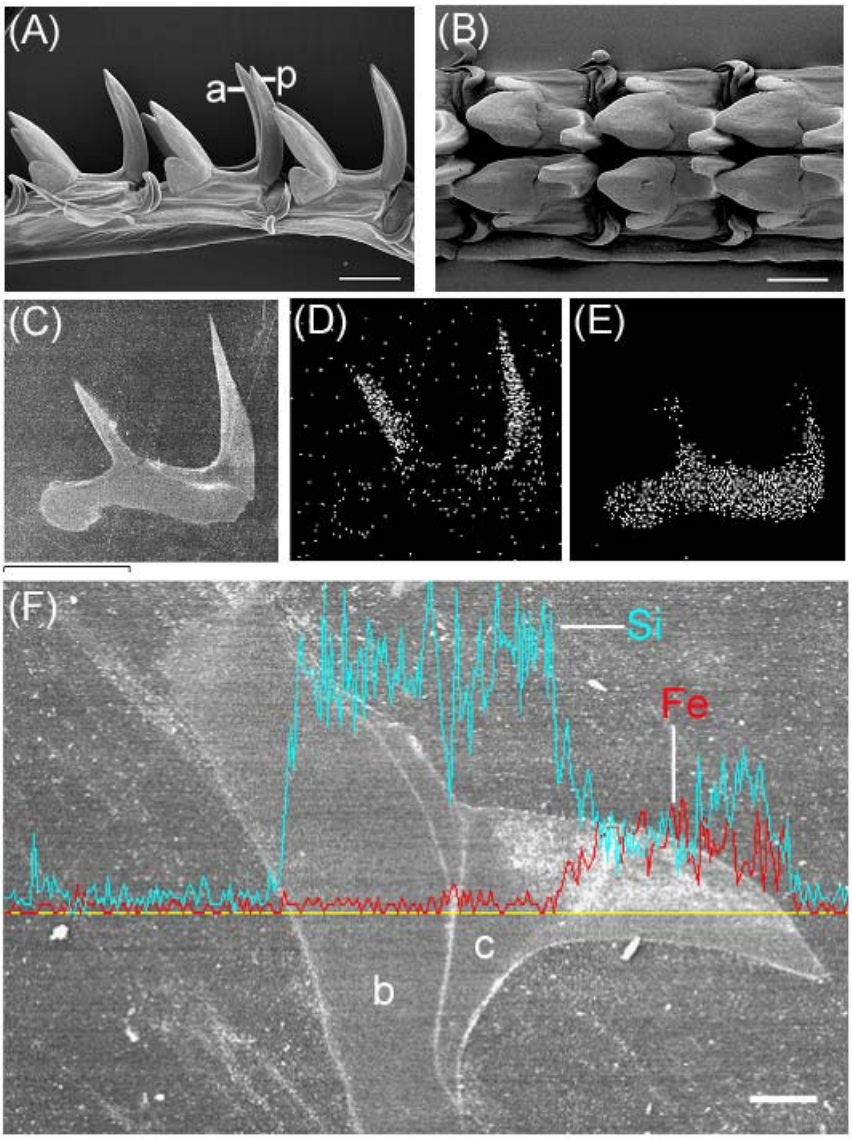


FIG. 4. Scanning electron microscope image and energy dispersive spectroscopy (EDS) qualitative elemental maps of the radula of *N. schrenckii*. (A) Side view; A, anterior end; P, posterior end. (B) Top view. (C) Secondary electron image of the embedded teeth. (D) Energy dispersive spectroscopy (EDS) map of Si in (C). (E) Energy dispersive spectroscopy (EDS) map of Fe in (C). (F) Line profile from tooth base to the anterior side of tooth cusp. The line along which the elemental analysis carried out is yellow; P, posterior end of the cusp; b, base; c, cusp. Scale bar, 100 μm.

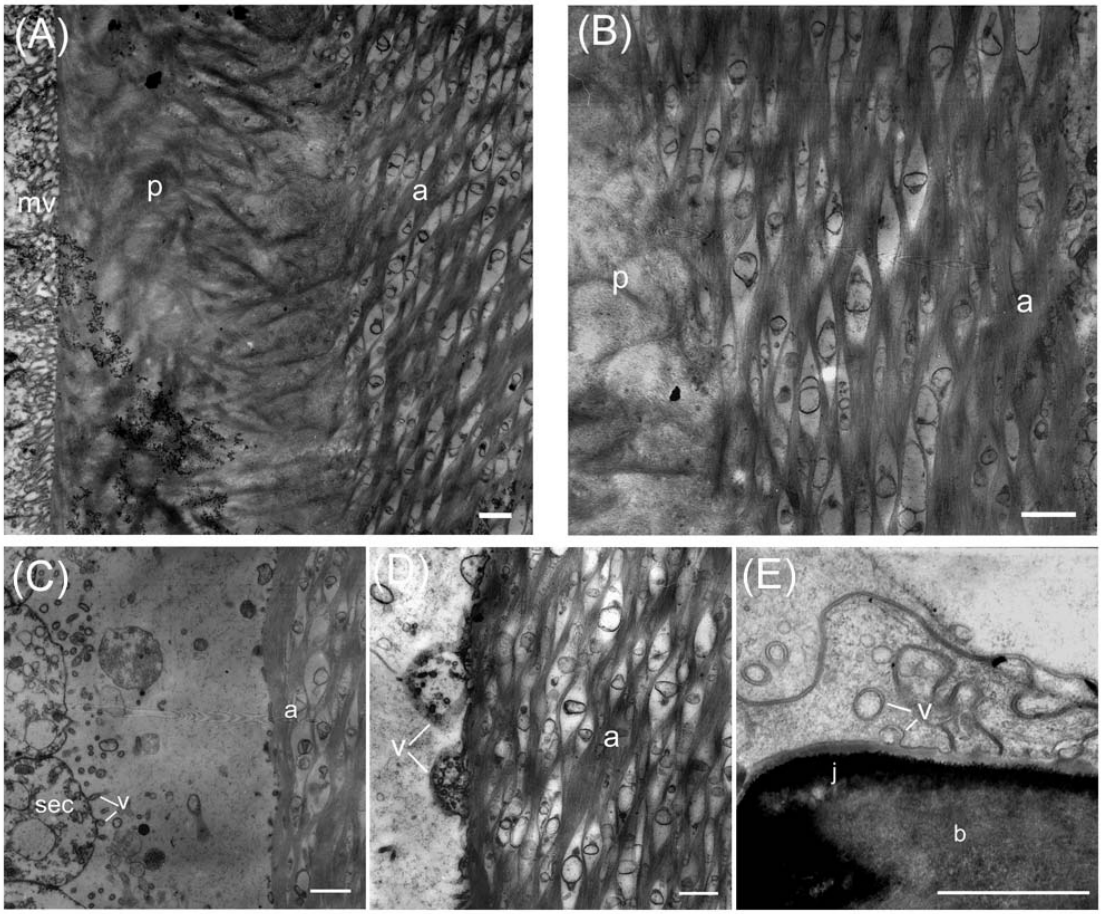


FIG.5. Transmission electron micrographs of sections of immature radular tooth cusp together with the surrounding epithelial cells. Scale bar, 1 μm.
(A) Unmineralized tooth cusp of early stage I; A, anterior side of tooth cusp; P, posterior side of cusp; mv, microvilli. (B) Further magnification of the interior of tooth cusp; A, anterior side of tooth cusp; P, posterior side of cusp. Note that at the anterior side, eye-shaped structures can be seen, which may be the residues of cells constituting the tooth cusp framework. (C) The anterior region of tooth cusp and the superior epithelial cells; A, anterior side of tooth cusp; sec, superior epithelial cell. Note that vesicles are budding from the epithelial cells (arrow). (D) Vesicles (arrow) fusing with the wall of anterior tooth cusp; A, anterior side of tooth cusp; v, vesicle. (E) Vesicular transportation can also be found between the tooth base and the cells adjacent to the anterior region of tooth cusp. Vesicles (arrow) were budding off from the tooth base; b, tooth base; v, vesicle; j, junction zone.

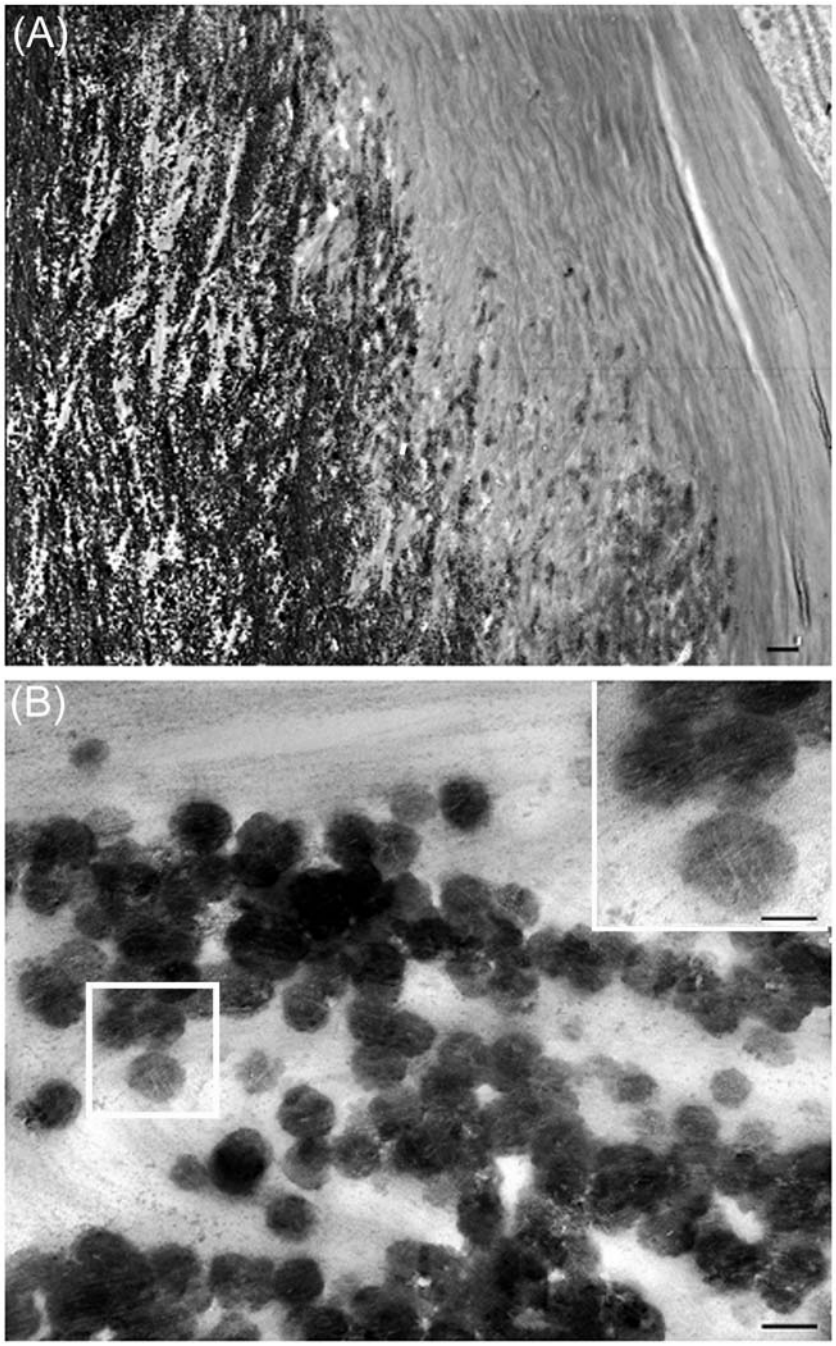


FIG. 6. (A) Transmission electron micrograph of the base of stage III radula. Spherical granules were observed. Scale bar, 1 μm (B) Magnified electron image of the granules. Scale bar, 100 nm Further magnification of the area indicated by the square is shown in inset A. Note the fine filaments run through the particles. Scale bar, 50 nm.

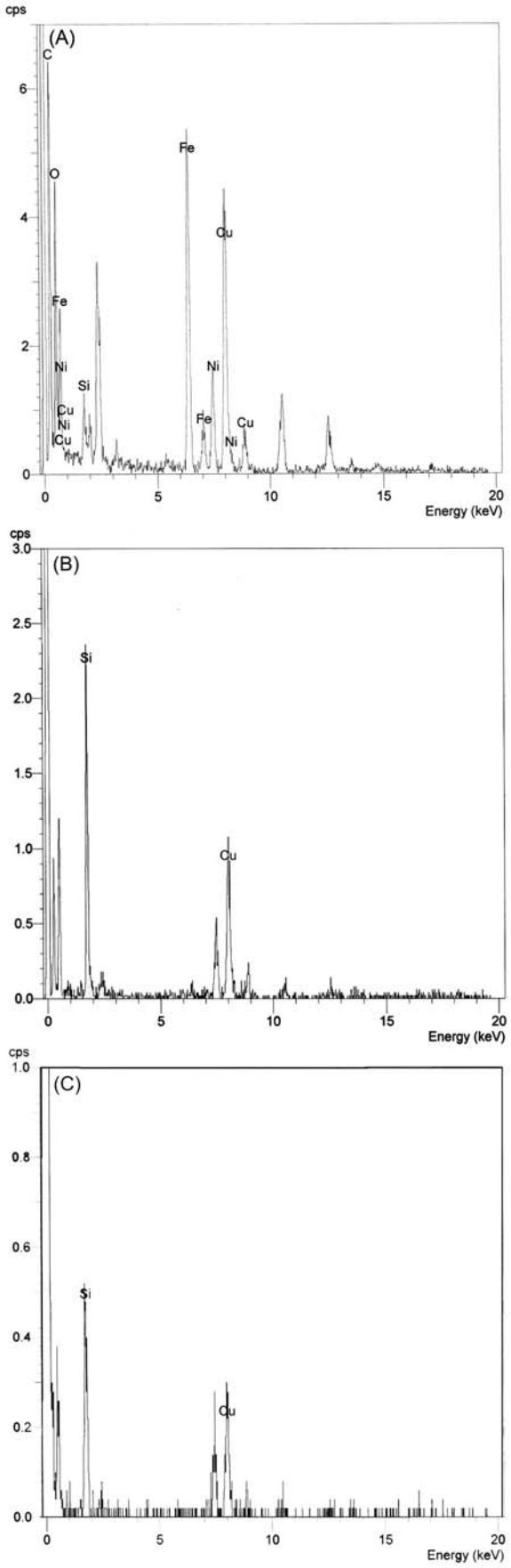


FIG. 7. TEM Energy-disperse X-ray analysis results of tooth ultrasection. (A) the junction zone; (B) tooth base; (C) spherical granules.

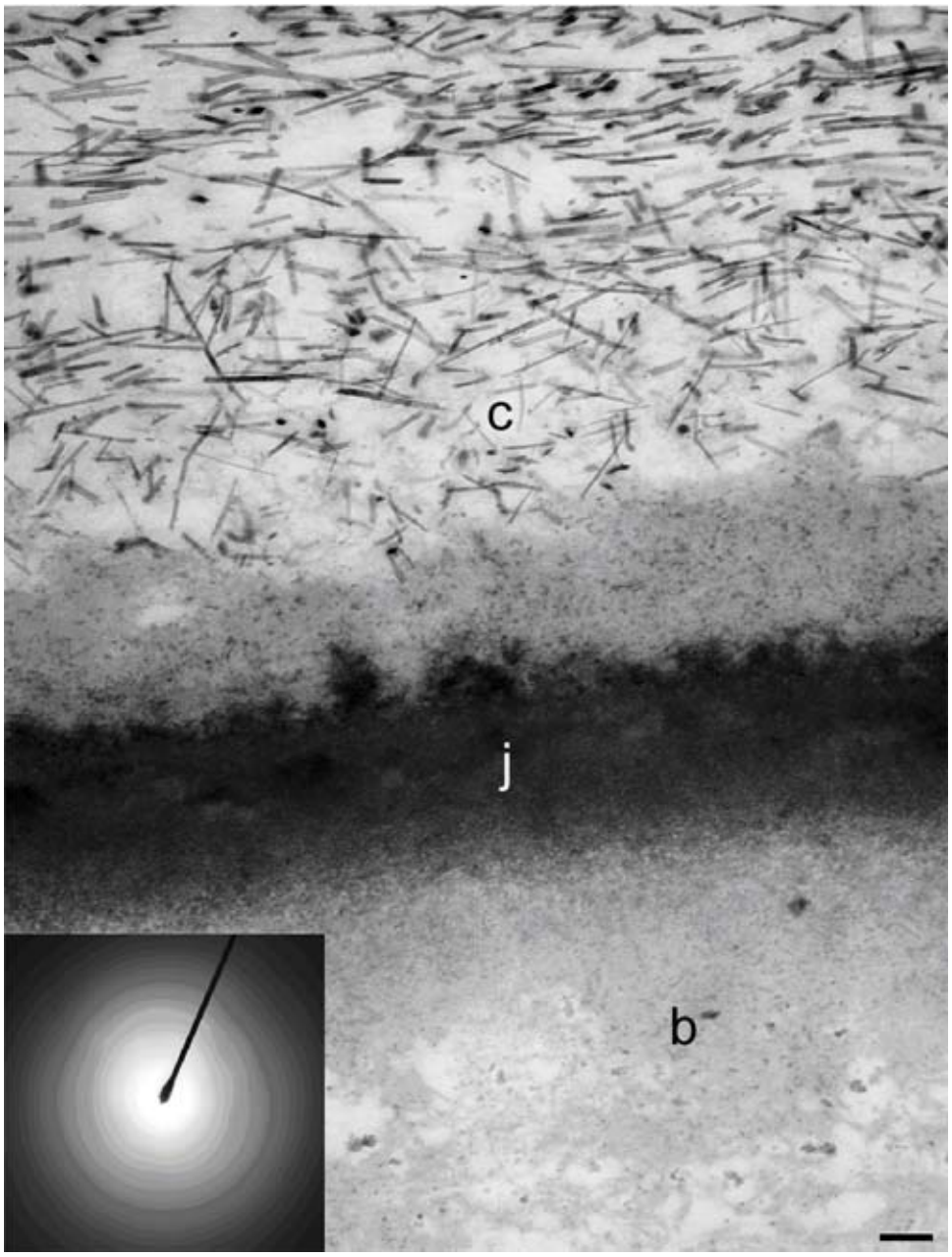


FIG. 8. TEM diffraction analysis of the radula ultramicrotome section. The analysis was focused in the junction zone, and the diffraction pattern suggests that there are no crystalline structure in this region (inset A); b, base; j, junction zone; c, cusp. Scale bar, 100 nm.

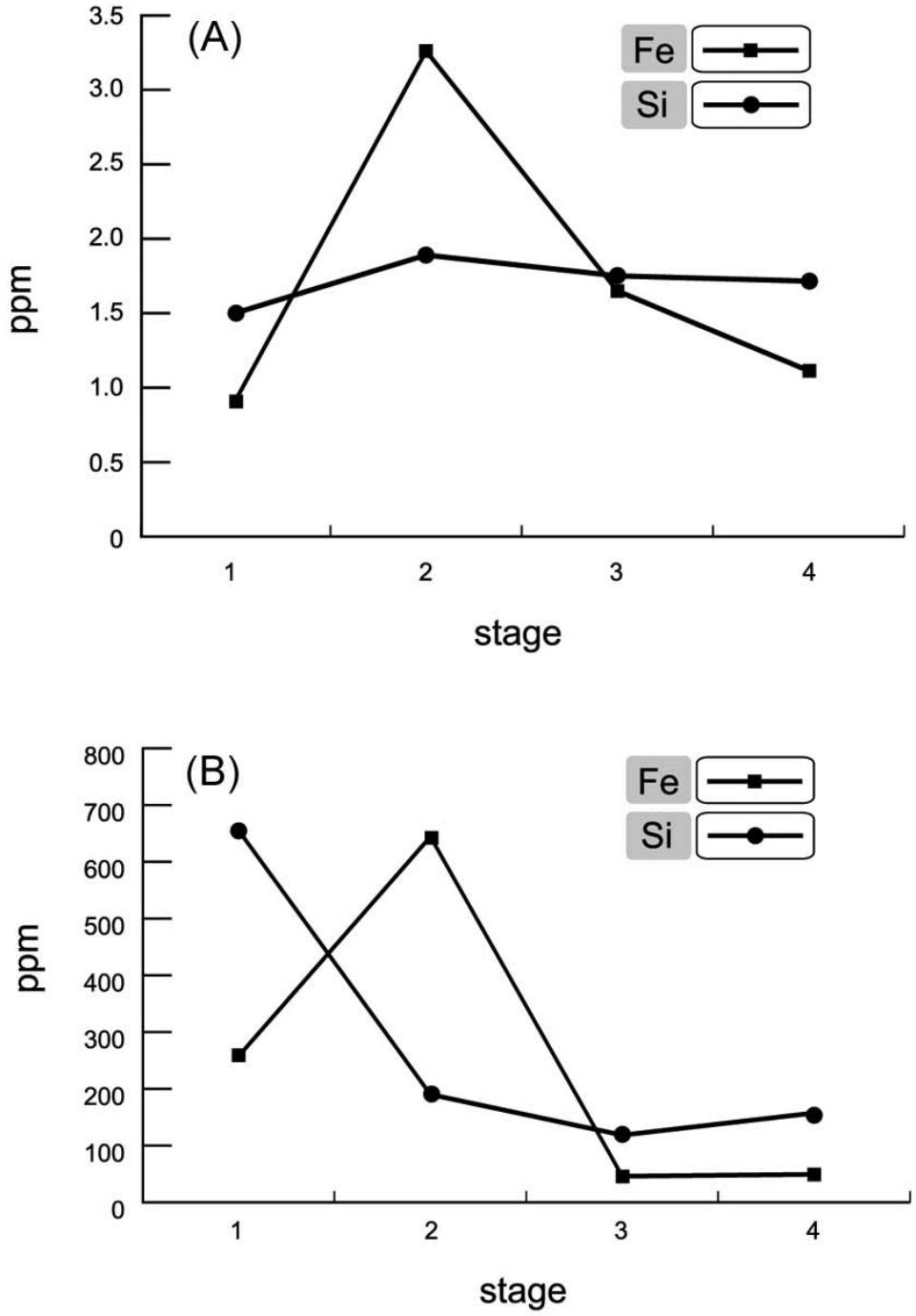


FIG. 9 ICP-MS analysis of soluble iron and silica contents in epithelial cells surrounding the radula (A), and the radula (B).

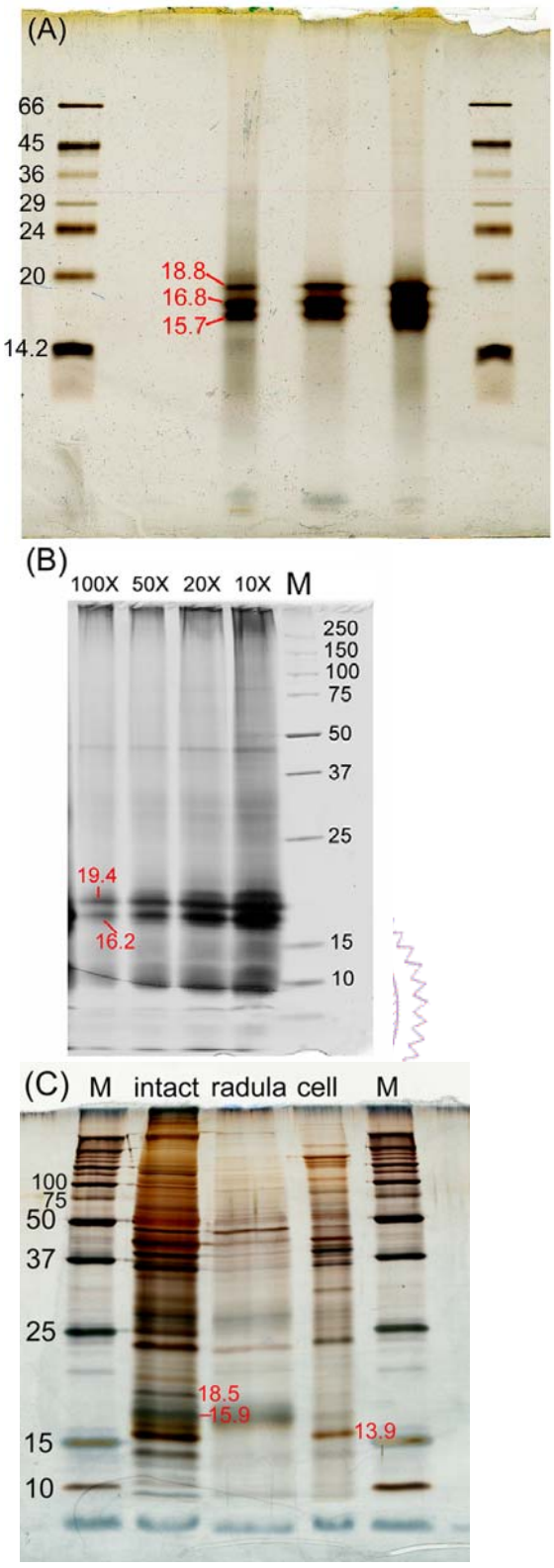


FIG. 10. Electrophoresis of peptides of interest differed in extraction sites and methods.

(A) Peptides extracted from cusps with 4 M HF/8 M $NH_4F$. (B) Peptides extracted with SDS-boiling method from the epithelial cells with different dilution. (C) Peptides extracted from the intact radulae with SDS-boiling; M, molecular weight marker.

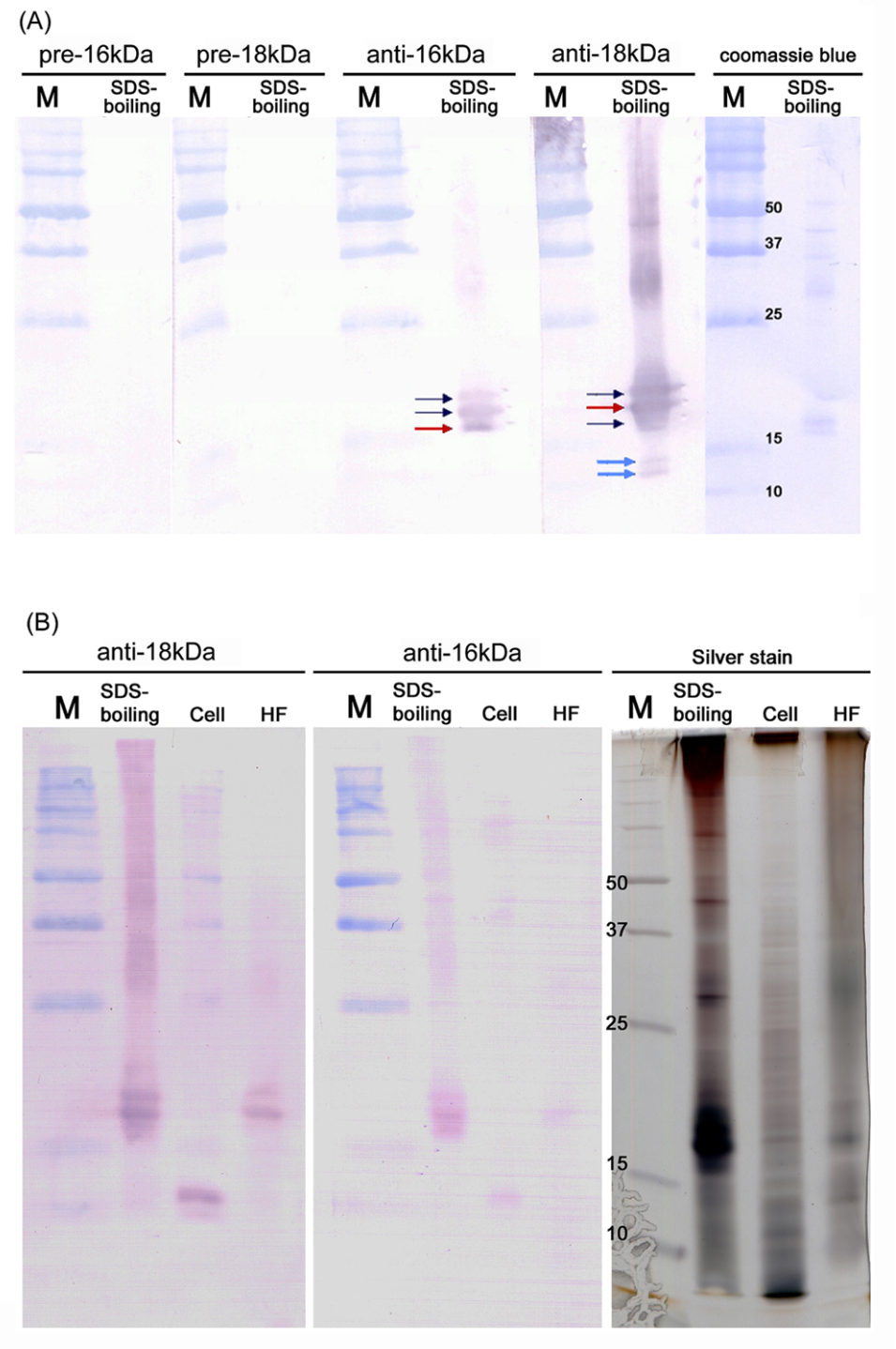


FIG. 11. Western blotting of anti-16 kDa and anti-18 kDa antibodies. (A) Test of specificity. The pre-immune serum and antibodies were both applied to the peptide extracted from epithelial cells with SDS-boiling. The antibodies were showed to exhibit specificity against peptides of interest. (B) Both anti-16 kDa and anti-18 kDa antibodies can recognize samples harvested from different source and extraction methods suggested that peptides within cusps might initially comes from the epithelial cells.

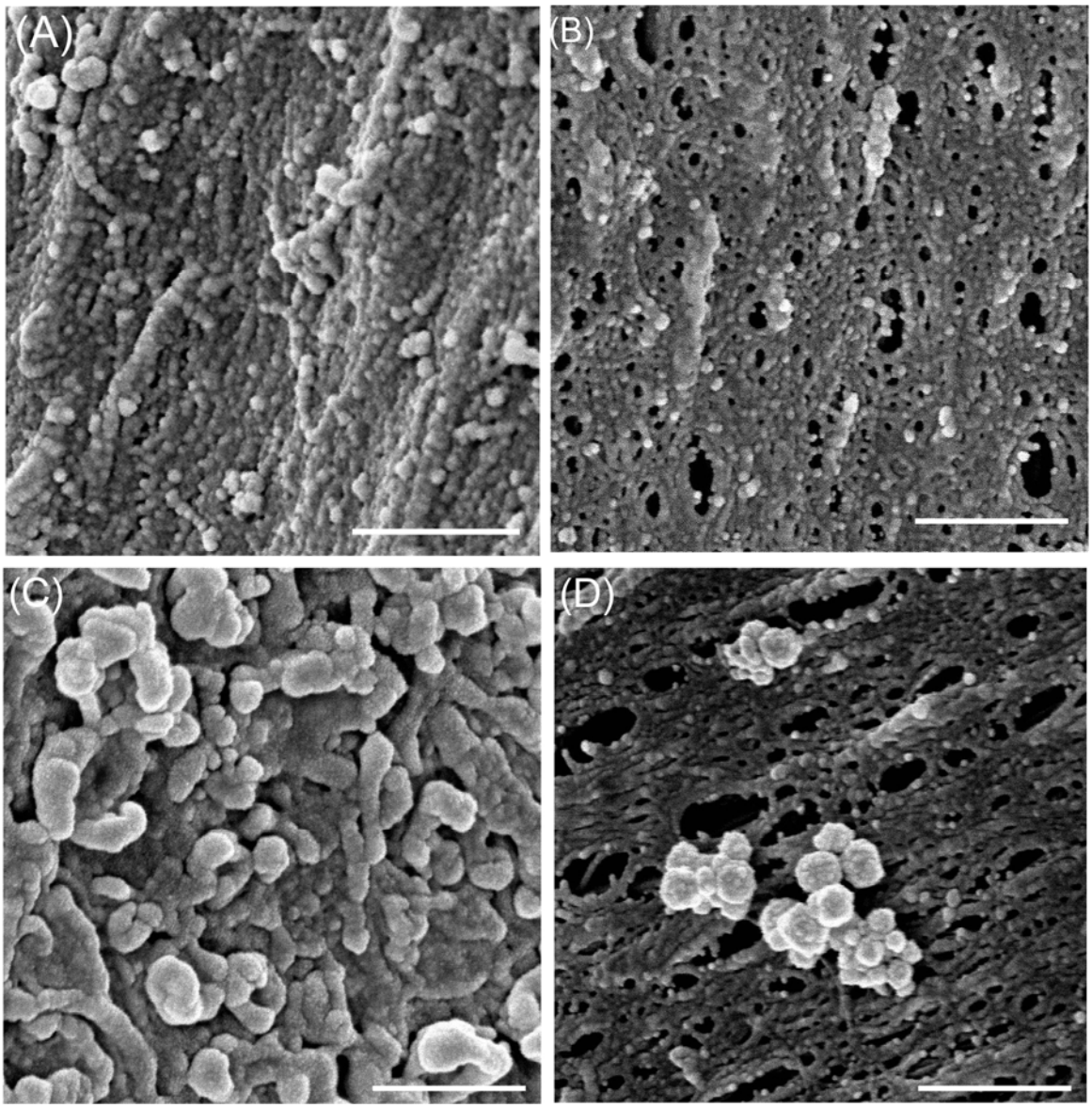


FIG. 12. SEM images silica re-deposition experiments. Scale bar, 500 nm. (A) Radula remained intact after removal of surrounding epithelial cells. Organized crystal structures can be seen from a broken tooth cusp. (B) Radulae treated only with $NH_4F$ to remove surface silica. The cusp surface observed became porous and no silica granule aggregation was observed. (C) Radulae treated with TEOS following $NH_4F$ treatment. Large amount of silica aggregation was seen on the cusp surface. (D) After gently remove the silica from the surface with $NH_4F$, radulae were subjected to TEOS treatment and then followed by $NH_4F$ treatment again. The SEM image shows that the cusp surface became porous, exhibiting morphology similar to that observed in (B), and granular aggregation of silica was observed.